Effective Thermal Properties of Multilayered Systems with Interface Thermal Resistance in a Hyperbolic Heat Transfer Model

J. Ordóñez-Miranda · J. J. Alvarado-Gil

Abstract One-dimensional thermal wave transport in multilayered systems with an interface thermal resistance is studied under the framework of the Cattaneo–Vernotte hyperbolic heat conduction model, considering modulated heat excitation under Dirichlet and Neumann boundary conditions. For a single semi-infinite layer, analytical formulas useful in the measurement of its thermal relaxation time as well as additional thermal properties are presented. For a composite-layered system, in the thermally thin regime, with the Dirichlet boundary condition, the well known effective thermal resistance formula is obtained, while for the Neumann problem, only the heat capacity identity is found. In contrast, in the thermally thick case, an analytical expression for both Dirichlet and Neumann conditions is obtained for the effective thermal diffusivity of the whole system in terms of the thermal properties of the individual layers and their interface thermal resistance. The limits of applicability of this equation, in the thermally thick regime, are shown to provide useful and simple results in the characterization of layered systems and that they can be reduced to the results obtained using the Fourier approach. The role of the thermal relaxation time, the interface thermal resistance, and the implications of these results in the possibility of enhancement in heat transport are discussed.

Keywords Effective thermal properties · Hyperbolic heat conduction · Layered system · Thermal properties determination · Thermal resistance

J. Ordóñez-Miranda · J. J. Alvarado-Gil (✉)
Applied Physics Department, Centro de Investigación y de Estudios Avanzados del I.P.N-Unidad Mérida, Carretera Antigua a Progreso km. 6, A.P. 73 Cordemex, 97310 Mérida, Yucatán, México
e-mail: jjag@mda.cinvestav.mx; jjag09@yahoo.com

J. Ordóñez-Miranda
e-mail: eordonez@mda.cinvestav.mx

1 Introduction

Effective models are useful tools in the understanding and practical predictions of the physical properties of heterogeneous materials [1]. In the case of heat transfer, those models are usually based on Fourier's law. This equation is supported by an impressive quantity of useful and successful results that show very good agreement with experimental data for most of the analyzed experimental conditions [2,3]. However, in recent experimental results on a variety of physical systems including nanofluids, different research groups have reported thermal conductivities much higher than the values expected from those previously observed and predicted by conventional mean field models based on Fourier's law. These results indicate that the validity of the basic heat transport equations must be revised [4–6].

It has been shown that the Fourier heat diffusion law predicts an infinite velocity for heat propagation, in such a way that a temperature change in any part of the material would result in an instantaneous perturbation at each point of the sample. This inconsistency has been studied by different researchers; comprehensive reviews containing different approaches to surmount Fourier equation limitations can be found in the literature [7,8]. The origin of this fundamental problem is due to the fact that the Fourier's law establishes explicitly that, when a temperature gradient at time t is imposed, the heat flux starts instantaneously at the same time t. Considering that heat transport is due to microscopic motion and collisions of particles, atoms, and molecules, it is straightforward to conclude that the Fourier condition on the velocity of heat transport cannot be sustained [7,9,10].

One of the simplest approaches to solve this problem was given by Cattaneo [11] and independently by Vernotte [12], who suggested to incorporate the finite propagation speed of heat while retaining the basic nature of Fourier's law, modifying the heat flux equation in the form,

$$q(x, t + \tau) = -k \frac{\partial T(x, t)}{\partial x}, \qquad (1)$$

where x is the spatial coordinate, t is the time, q (W$\cdot$m^{-2}) is the heat flux, T (K) is the absolute temperature, k (W$\cdot$m$^{-1}\cdot$K^{-1}) is the thermal conductivity, and τ (s) is the thermal property of the medium known as the thermal relaxation time, which represents the time necessary for the initiation of the heat flux after a temperature gradient has been imposed at the boundary of the medium. Equation 1 establishes that the heat flux does not start instantaneously, but rather grows gradually with the thermal relaxation time after the application of the temperature gradient. Conversely, τ represents the time necessary for the disappearance of the heat flux after the removal of the temperature gradient [10,13]. In this way Eq. 1 establishes explicitly that the temperature gradient always precedes the heat flux. A generalization of Fourier's law and of Eq. 1 has also been proposed by Tzou [8,14,15], who establishes that either the temperature gradient may precede the heat flux or the heat flux may precede the temperature gradient, by incorporating one time delay in the heat flux and one in the temperature gradient. These models have been shown to be admissible by the second law of extended irreversible thermodynamics [8] and by the Boltzmann

transport equation [16]. In order to establish the impact of the possible generalizations of Fourier's law on the concepts and values of effective thermal properties, it is of main importance to develop adequate methodologies and equations using the Cattaneo–Vernotte (CV) approach. The predictions of the effective thermal properties by more realistic models than the CV model should be in agreement with the results predicted by the hyperbolic model, in the appropriate limit.

Assuming that the thermal relaxation time is much shorter that the typical response time in a transient process ($\tau \ll t$), Eq. 1 can be approximated by a first-order Taylor series expansion, as follows:

$$q\left(x,t\right) + \tau \frac{\partial q\left(x,t\right)}{\partial t} = -k \frac{\partial T\left(x,t\right)}{\partial x}, \tag{2}$$

whose solution is given by

$$q\left(x,t\right) = -\frac{k}{\tau} \mathrm{e}^{-t/\tau} \int\limits_{-\infty}^{t} \mathrm{e}^{\eta/\tau} \frac{\partial T\left(x,\eta\right)}{\partial x} \mathrm{d}\eta. \tag{3}$$

In this way, Eq. 3 establishes that the heat flux $q(x,t)$ at a certain time t depends on the history of the temperature gradient established in the whole time interval from $-\infty$ to t. This indicates that the heat flux has thermal memory, a consequence of the finite value of the thermal relaxation time [17]. In this way, Eq. 3 predicts a dependence of the time path of the temperature gradient rather than an instantaneous response predicted by the Fourier law.

In order to uncouple the variables q and T, Eq. 2 has to be combined with the energy conservation equation established at time instant t, given by [2]

$$\frac{\partial q(x,t)}{\partial x} + \rho c \frac{\partial T(x,t)}{\partial t} = S(x,t), \tag{4}$$

where ρ $(\mathrm{kg} \cdot \mathrm{m}^{-3})$ is the density, c $(\mathrm{J} \cdot \mathrm{kg}^{-1} \cdot \mathrm{K}^{-1})$ is the specific heat of the medium, and the source term S $(\mathrm{W} \cdot \mathrm{m}^{-3})$ represents the rate per unit volume at which the heat flux is generated. Combining Eqs. 2 and 4, and assuming constant thermal properties in such a way that they are independent of the position, the hyperbolic heat conduction equation is obtained [7,18];

$$\frac{\partial^2 T(x,t)}{\partial x^2} - \frac{1}{\alpha} \frac{\partial T(x,t)}{\partial t} - \frac{\tau}{\alpha} \frac{\partial^2 T(x,t)}{\partial t^2} = -\frac{1}{k} \left(S(x,t) + \tau \frac{\partial S(x,t)}{\partial t} \right), \tag{5}$$

where $\alpha = k/(\rho c)$ is the thermal diffusivity of the medium of concern. On the left-hand side of Eq. 5, the second-order time derivative term indicates that heat propagates as a wave with a characteristic speed $\sqrt{\alpha/\tau}$ and the first-order time derivative term corresponds to a diffusive process, which is damping spatially the heat wave. Notice that Eq. 5 reduces to the parabolic heat conduction equation (based on Fourier's law) for $\tau \to 0$ or in a steady-state condition $\partial \vec{J}(\vec{x},t)/\partial t = 0$. In this way the CV equation

incorporates the finite speed of heat propagation while retaining the basic nature of Fourier's law.

The applicability of the CV equation has been widely discussed [6,7,19,20]. It is clear that a physical system would follow the predicted hyperbolic behavior if the time scale of the heat transport phenomenon analyzed is of the order of the thermal relaxation time. This quantity is associated with the average communication time among the collisions of electrons and phonons, and its reported values for metals, superconductors, and semiconductors are of the order of microseconds (10^{-6} s) to picoseconds (10^{-12} s) [10]. These small values of the thermal relaxation time indicate that its effects will not be significant if the physical time scales are of the order of microseconds or larger. In these situations Fourier equation provides an adequate approach. However, in modern applications such as in analysis and processing of materials using ultrashort laser pulses and high speed electronic devices, the finite value of the relaxation time is necessary to be considered [6,17,19–21].

One of the most interesting questions is the applicability of the hyperbolic formalism in what is known as materials with a non-homogeneous inner structure, such as biological tissues, granular materials, and nanofluids. For these systems, several authors have claimed that they have measured hyperbolic effects with thermal relaxation times of the order of seconds [6,18,20,22]. It is expected that the CV equation could provide effective thermal properties, due to the fact that in a hyperbolic model, heat transport behaves more wave-like than in the traditional Fourier parabolic approach [7].

Layered structures are among the best studied non-homogenous systems and constitute one of the basic configurations for the analysis and development of effective thermal properties models [1]. These systems have been studied in stationary and in dynamic heat transfer conditions [23–28]. By using the CV equation, Khadrawi et al. [25] and Lor and Chu [29] have studied the thermal behavior of a two-layer system with perfect and imperfect thermal contact. These authors have shown that the interface thermal resistance as well as the thermal relaxation time play a determinant role in the thermal response of the system. In addition, the thermal behavior of a layered system under the framework of the dual-phase lagging model of heat conduction [8,18], has also been investigated by various research groups [8,18,30–34]. Recently, Ramadan et al. [31–34] have studied the thermal behavior of the layers in the absence and presence of the interface thermal resistance. They have found that the effect of the thermal contact between the layers is very important in the transient process of heat transfer.

When a material is excited by a modulated heat source, a train of thermal waves is generated, with its transport determined by the thermal properties, the boundary conditions, as well as the geometry of the physical system. This area of research has provided useful and meaningful results for interpretation of heat diffusion and transport using Fourier's law [26,28,35–37]. In this case it has been shown that, depending on the thermal wave penetration inside the material, the effective thermal properties could show a complex behavior influenced by the modulation frequency of the heating source [26,28]. The generalization of this approach for two-layer systems under the hyperbolic heat transport equation has been studied [38]; however, the role of the interface thermal resistance as well as the thermal relaxation time on the effective thermal properties has not been fully explored.

In this work, it will be shown that the values of the effective thermal diffusivity in a layered system, in the scheme of hyperbolic heat transport, depend crucially not only on the traditional thermal properties of the layers such as thermal diffusivity, thermal conductivity, thermal effusivity, and thermal interface resistance, but also on the thermal relaxation time. In addition, it provided a straightforward methodology to evaluate the value of the effective thermal relaxation time and its role in different modulation frequency ranges.

2 Mathematical Formulation and Solutions

Let us consider the configuration shown in Fig. 1, in which the system is excited externally at the surface $x = 0$ by either a modulated temperature $T(x = 0, t)$ or heat source $S(x = 0, t)$ at frequency f of the form [39,40],

$$T(x = 0, t) = \Theta (1 + \cos(\omega t)) = \text{Re}\left[\Theta\left(1 + e^{i\omega t}\right)\right], \tag{6a}$$

$$S(x = 0, t) = Q (1 + \cos(\omega t)) = \text{Re}\left[Q\left(1 + e^{i\omega t}\right)\right], \tag{6b}$$

where $\omega = 2\pi f$, $\text{Re}(\xi)$ is the real part of and Θ (K) and Q (W·m^{-3}) are two positive constants. For any of these thermal excitations, the temperature at any point of the sample is given by

$$T(x, t) = T_{\text{amb}} + T_{\text{dc}}(x) + T_{\text{ac}}(x, t), \tag{7}$$

where T_{amb} corresponds to the ambient temperature, $T_{\text{dc}}(x)$ and $T_{\text{ac}}(x, t) = \text{Re}\left[\theta(x)e^{i\omega t}\right]$ are the stationary raising and periodic components of the temperature; these last two terms are due to the first and second terms of the corresponding thermal excitations, respectively. From now on, the operator Re() will be omitted, taking into
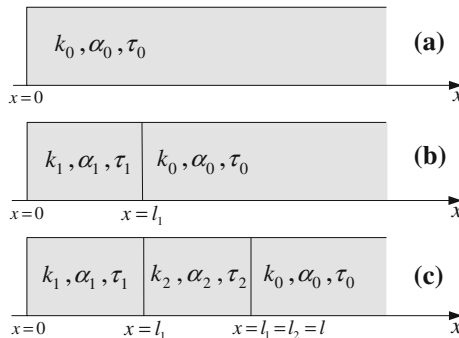

Fig. 1 Schematic diagram of the studied layered systems: (a) semi-infinite one-dimensional sample of thermal conductivity k_0, thermal diffusivity α_0, and relaxation time τ_0; (b) a layer of thermal conductivity k_1, thermal diffusivity α_1, relaxation time τ_1, and thickness l_1 is added to the semi-infinite system of (a); and (c) an additional layer of thermal conductivity k_2, thermal diffusivity α_2, relaxation time τ_2, and thickness l_2 is inserted between the two layers of the previous system

account the convention that the real part of the expressions of the temperature must be taken to obtain physical quantities. Our attention will be focused on the spatial component [$\theta(x)$] of the oscillatory part of the temperature, due to the fact that it is the quantity of interest in lock-in and similar detection techniques.

Inserting Eq. 7 into Eq. 5 and considering that there are no any internal heat sources, then for $x \geq 0$, the general solution of Eq. 5 for $\theta(x)$ is given by

$$\theta(x) = Be^{px} + Ce^{-px}, \tag{8}$$

where B and C are two constants that depend on the boundary conditions at $x = 0, l_1, l$ of the corresponding problem and p is given by

$$p = \sqrt{\frac{i\omega}{\alpha}}\sqrt{1 + i\omega\tau} = \frac{\chi + i\chi^{-1}}{\mu}, \tag{9a}$$

$$\mu = \sqrt{\frac{2\alpha}{\omega}} = \sqrt{\frac{\alpha}{\pi f}}, \tag{9b}$$

$$\chi = \sqrt{\sqrt{1 + (\omega\tau)^2} - \omega\tau}. \tag{9c}$$

It is important to observe that for low frequencies ($\omega\tau \ll 1$) the parameter χ tends to unity and the parameter p approaches its classical value $p_c = (1 + i)/\mu$ [16,17]. On the other hand, for high frequencies ($\omega\tau \gg 1$), the parameter χ tends to $1/\sqrt{2\omega\tau}$ and the parameter $p \to (1 + i2\omega\tau)/2\sqrt{\alpha\tau}$, whose real part is independent of the modulation frequency and, therefore, it predicts that the hyperbolic thermal waves are able to travel larger distances than the parabolic ones predicted by Fourier's law. Notice that, in general, the hyperbolic thermal conduction length, μ_h, analogous to the parabolic thermal diffusion length μ, is given by

$$\mu_h = \frac{\mu}{\chi}, \tag{10}$$

This corresponds to the distance at which the amplitude of the hyperbolic thermal wave falls to a value $e^{-1} \approx 0.368$ of its size at the surface ($x = 0$). In Fig. 2, the behavior of the hyperbolic thermal conduction length as functions of the modulation frequency is shown for three different values of the thermal relaxation time. The parabolic thermal diffusion length is shown in the same figure by a dashed line.

Figure 2 shows that when the frequency decreases ($\omega\tau \ll 1$), the thermal conduction length reduces to the one predicted by the parabolic model. In contrast, for high frequencies ($\omega\tau \gg 1$), the parabolic thermal diffusion length reduces to zero while the hyperbolic thermal conduction length tends to a value $\left(=2\sqrt{\alpha\tau}\right)$ independent of the modulation frequency. For a constant value of the thermal diffusivity, this last value is larger when the thermal relaxation time increases. Since the hyperbolic thermal conduction length for any frequency is larger than the parabolic thermal diffusion length, the hyperbolic thermal waves are less attenuated than the parabolic ones.
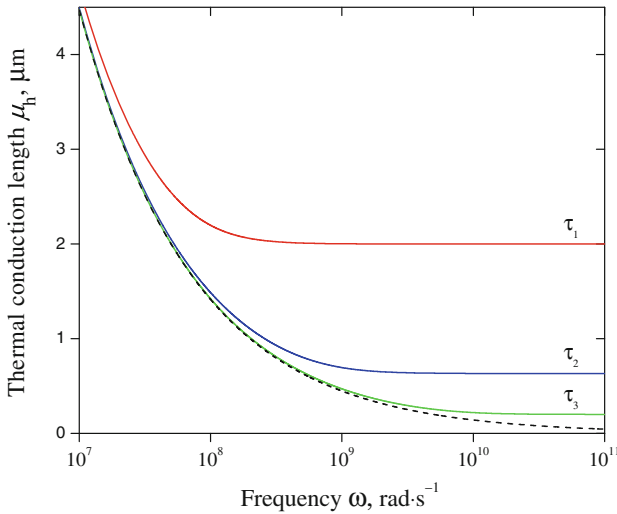
Fig. 2 Thermal conduction length as a function of the modulation frequency. The *dashed line* corresponds to the parabolic model and the *solid lines* to the hyperbolic approach for three values of the thermal relaxation time: $\tau_1 = 10^{-8}$ s, $\tau_2 = 10^{-9}$ s, and $\tau_3 = 10^{-10}$ s; and taking $\alpha = 1 \times 10^{-4}$ m$^2 \cdot$ s^{-1}

Considering that there is a thermal resistance R (m$^2 \cdot$ K $\cdot$ W^{-1}) at the interface of the layers [41,42], the boundary conditions obtained from the usual requirement of the temperature discontinuity and heat flux continuity at the interfaces $x = l_1, l$ are given by

$$\theta(x^-) - \theta(x^+) = \frac{R^{\pm} k\left(x^+\right)}{1 + i\omega\tau^+} \frac{\mathrm{d}\theta\left(x^+\right)}{\mathrm{d}x}, \tag{11a}$$

$$\frac{k(x^-)}{1 + i\omega\tau^-} \frac{\mathrm{d}\theta(x^-)}{\mathrm{d}x} = \frac{k\left(x^+\right)}{1 + i\omega\tau^+} \frac{\mathrm{d}\theta\left(x^+\right)}{\mathrm{d}x}, \tag{11b}$$

where the superscripts "+" and "−" indicate that the limit $x \to l_1$ ($x \to l$) is taken from the right and left of the point $x = l_1$ ($x = l$), respectively. The form of Eqs. 11a and 11b may be derived using Eqs. 2 or 3. In what follows, the explicit solutions given by the two types of excitations represented in Eqs. 6a, 6b are obtained.

2.1 Dirichlet Problem

In this case, according to Eq. 6a, the following boundary condition is considered:

$$\theta(x = 0) = \Theta, \tag{12}$$

2.1.1 Semi-Infinite Layer (Fig. 1a)

In this case the physically acceptable solution goes to zero for large distances $[\theta(x \to \infty) \to 0]$ and according to Eqs. 8 and 12 is given by

$$\theta(x) = \Theta e^{-p_0 x}, \qquad (13)$$

where p_0 is defined by Eqs. 9a–9c for the thermal properties of the semi-infinite layer (layer 0) and $x \geq 0$.

2.1.2 Semi-Infinite Layer in Contact with the Layer of Thickness l_1 (Fig. 1b)

Using Eqs. 8, 11a, 11b, and 12, it is obtained that the solution for the spatial part of the thermal wave and for $x \geq l_1$ is given by

$$\theta(x) = \frac{2\Theta}{(1 + \lambda_{01} + R_{10}\lambda_0)e^{p_1 l_1} + (1 - \lambda_{01} + R_{10}\lambda_0)e^{-p_1 l_1}} e^{-p_0(x-l_1)}, \qquad (14)$$

where p_1 is defined by Eqs. 9a–9c for the thermal properties of the first layer (layer 1), R_{10} is the interface thermal resistance between layers 1 and 0, and $\lambda_{01} = \lambda_0/\lambda_1$ with

$$\lambda_j = \frac{\varepsilon_j \sqrt{i\omega}}{\sqrt{1 + i\omega\tau_j}}, \qquad (15)$$

and with $\varepsilon_j = k_j/\sqrt{\alpha_j}$ being the thermal effusivity of the layer $j = 0, \ 1$. This thermal property measures the ability of the materials to exchange heat with its surroundings [43].

2.2 Two Finite Layers in Contact with a Semi-Infinite Layer (Fig. 1c)

In this case for $x \geq l$, the solution obtained using Eqs. 8, 11a, 11b, and 12 is

$$\theta(x) = \frac{4\Theta\eta_1\eta_2}{D} e^{-p_0(x-l)}, \qquad (16)$$

where

$$D = (\eta_1^2 + 1)\xi_1 + \lambda_{01}(\eta_1^2 - 1)\xi_2, \qquad (17a)$$

$$\xi_1 = (\eta_2^2 + 1)[1 + (R_{12} + R_{20})\lambda_0] + (\eta_2^2 - 1)[\lambda_{02} + R_{12}\lambda_2(1 + R_{20}\lambda_0)], \qquad (17b)$$

$$\xi_2 = (\eta_2^2 + 1) + (\eta_2^2 - 1)(\lambda_{20} + R_{20}\lambda_2), \qquad (17c)$$

$$\eta_j = e^{q_j l_j}, \quad j = 1, 2. \qquad (17d)$$

$$\lambda_j = \frac{\varepsilon_j \sqrt{i\omega}}{\sqrt{1 + i\omega\tau_j}}, \quad j = 0, 1, 2. \qquad (17e)$$

$$\lambda_{jn} = \lambda_j/\lambda_n, \quad j, n = 0, 1, 2. \qquad (17f)$$

2.3 Neumann Problem

Considering that the optically opaque surface [39] of a material is uniformly illuminated by a laser light beam of periodically modulated intensity, the heat source is given by [39,40]: $I_0 [1 + \cos(\omega t)]/2 = \mathrm{Re}\left[I_0\left(1 + \mathrm{e}^{\mathrm{i}\omega t}\right)\Big/2\right]$, where $I_0 = F\eta(1 - R)I$, with F a parameter determined by the optical, thermal, and geometric properties of the first layer, η is the efficiency at which the absorbed light is converted into heat, R is the reflection coefficient of the surface at $x = 0$, and I $(\mathrm{W \cdot m}^{-2})$ is the intensity of the light beam. Considering that the sample is illuminated with a fixed light source, the factor I_0 can be taken as nearly constant and independent of the modulation frequency as is usually assumed in similar problems [37,39]. The external boundary condition in this case has the following form:

$$-\left.\frac{k}{1 + \mathrm{i}\omega\tau}\frac{\mathrm{d}\theta\,(x)}{\mathrm{d}x}\right|_{x=0} = \frac{I_0}{2}. \tag{18}$$

Using Eqs. 8, 11a, 11b, and 18, the following results are obtained:

2.3.1 Semi-Infinite Layer (Fig. 1a)

In this case for $x \geq 0$, the temperature is given by

$$\theta(x) = \frac{I_0}{2\varepsilon_0}\frac{\sqrt{1 + \mathrm{i}\omega\tau_0}}{\sqrt{\mathrm{i}\omega}}\mathrm{e}^{-p_0 x}, \tag{19}$$

where all parameters have been defined previously.

2.3.2 Semi-Infinite Layer in Contact with the Layer of Thickness l_1 (Fig. 1b)

In this case for $x \geq l_1$, it is obtained that

$$\theta(x) = \frac{I_0}{2\varepsilon_1}\frac{\sqrt{1 + \mathrm{i}\omega\tau_1}}{\sqrt{\mathrm{i}\omega}}$$
$$\times\frac{1}{(1 + \lambda_{01} + R_{10}\lambda_0)\mathrm{e}^{p_1 l_1} - (1 - \lambda_{01} + R_{10}\lambda_0)\mathrm{e}^{-p_1 l_1}}\mathrm{e}^{-p_0(x - l_1)}, \tag{20}$$

where all parameters have been defined previously.

2.3.3 Two Finite Layers in Contact with a Semi-Infinite Layer (Fig. 1c)

It can be shown that for $x \geq l$, the temperature is given by

$$\theta(x) = \frac{I_0}{2\varepsilon_1}\frac{\sqrt{1 + \mathrm{i}\omega\tau_1}}{\sqrt{\mathrm{i}\omega}}\frac{4\eta_1\eta_2}{N}\mathrm{e}^{-p_0(x - l)}, \tag{21}$$

where

$$N = (\eta_1^2 - 1)\xi_1 + \lambda_{01}(\eta_1^2 + 1)\xi_2, \tag{22}$$

and all the other terms have been previously defined.

3 Results

In this section, useful formulas to determine the thermal properties, under the framework of the CV model of heat conduction, are obtained and analyzed.

3.1 Thermal Properties of a Semi-Infinite Layer

3.1.1 Dirichlet Problem

After expressing $\theta(x)$ as a complex function in its polar form, both its amplitude A and phase ϕ can be obtained, which for the case of the semi-infinite layer (Eq. 12) are

$$A = \Theta e^{-\sqrt{\pi f}\frac{x\chi_0}{\sqrt{\alpha_0}}}, \tag{23a}$$

$$\phi = -\sqrt{\pi f}\frac{x\chi_0^{-1}}{\sqrt{\alpha_0}}, \tag{23b}$$

The behavior of the normalized amplitude and phase as functions of the modulation frequency are shown in Fig. 3a and b, respectively; for two values of the thermal relaxation time ($\tau_0 = 1\times10^{-8}$ s, 1×10^{-9} s), which are characteristic of semiconductors [10]. It is assumed that the measurement is performed at $x = 2\times10^{-6}$ m and that the thermal diffusivity of the semi-infinite layer is $\alpha = 1\times10^{-4}$ m$^2\cdot$s^{-1}. The corresponding spectra, predicted by the parabolic model ($\tau_0 = 0$), are shown in the same figure by dashed lines.

In Fig. 3a and b, it is observed that when the frequency decreases ($\omega\tau_0 \ll 1$) the spectrum predicted by the hyperbolic model reduces to the one predicted by the parabolic model. In contrast, for high frequencies ($\omega\tau_0 \gg 1$), the behavior predicted by the parabolic model differs remarkably from the hyperbolic one. In fact, for sufficiently high frequencies, the normalized amplitude predicted by the parabolic model falls to zero while the one predicted by the hyperbolic model tends to a frequency-independent value, which is larger for larger thermal relaxation times.

By combining Eqs. 23a and 23b, it can be shown that

$$\alpha_0 = \frac{\pi f x^2}{\phi \ln(A/\Theta)}, \tag{24}$$

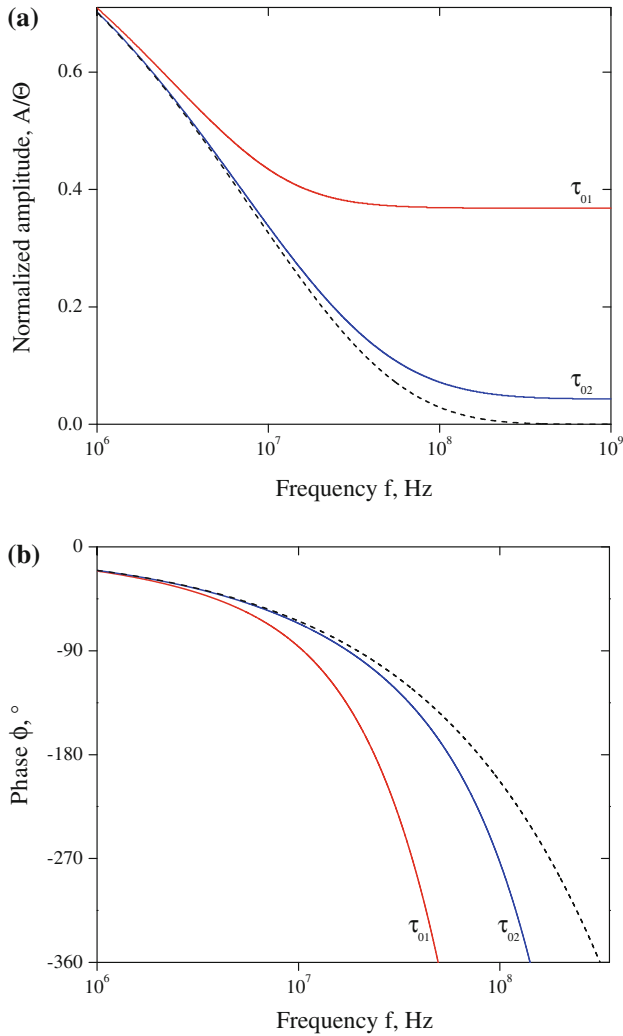$$\tau_0 = \frac{a^{-1} - a}{4\pi f}, \tag{25}$$

Fig. 3 (a) Normalized amplitude and (b) phase of the temperature as functions of the modulation frequency, for the Dirichlet problem and taking $x = 2 \times 10^{-6}$ m and $\alpha_0 = 10^{-4}$ m$^2 \cdot$ s^{-1}. The *dashed line* corresponds to the parabolic model and the *solid lines* to the hyperbolic equation, for two values of $\tau_0 : \tau_{01} = 1 \times 10^{-8}$ s, $\tau_{02} = 1 \times 10^{-9}$ s

where $a = \ln(A/\Theta)/\phi$ is smaller than unity, because the parameter χ is also smaller than unity. Equations 24 and 25 agree with the results obtained by Roetzel et al. [19] for the hyperbolic approach. In this way the thermal diffusivity and thermal relaxation time can be determined simultaneously by recording the amplitude and phase at some modulation frequency f and at a certain position x. Notice that in the parabolic model, $a = 1$ and therefore $\tau_0 = 0$.

3.1.2 Neumann Problem

The amplitude A and phase ϕ of the thermal signal expressed in Eq. 19 are given by

$$A = \frac{I_0}{2\varepsilon_0\sqrt{2\pi f}}\sqrt[4]{1+(2\pi f\tau_0)^2}\,e^{-\sqrt{\pi f}\frac{x\chi_0}{\sqrt{\alpha_0}}}, \tag{26a}$$

$$\phi + \frac{\pi}{4} = -\sqrt{\pi f}\frac{x\chi_0^{-1}}{\sqrt{\alpha_0}} + \frac{1}{2}\arctan(2\pi f\tau_0), \tag{26b}$$

The behavior of the normalized amplitude and phase as functions of the modulation frequency are shown in Fig. 4a and b, respectively, for the same data used in Fig. 3a. The corresponding spectra predicted by the parabolic model ($\tau_0 = 0$) are shown in the same figure by dashed lines. In Fig. 4a and b, it can be noticed that the spectra predicted by the hyperbolic and parabolic models are similar to those presented in Fig. 3a and b, respectively.

If the amplitude A and the phase ϕ are measured in an experiment, by performing a fitting procedure by means of Eq. 26b, both the thermal diffusivity (α_0) and the thermal relaxation time (τ_0) can be determined. Then using Eq. 26a, the thermal effusivity (ε_0) can also be obtained. Finally, the thermal conductivity of the semi-infinite layer is obtained using the relation, $k_0 = \varepsilon_0\sqrt{\alpha_0}$.

It is important to note that in the Neumann problem we have $b \equiv (\ln A)'/\phi' = \chi_0^2$, where the prime indicates a derivative with respect to x. After solving this equation for the thermal relaxation time, the following equation is obtained:

$$\tau_0 = \frac{b^{-1} - b}{4\pi f}, \tag{27}$$

which is analogous to Eq. 25 in the Dirichlet problem and can also be used to determine τ_0.

It is important to observe that under the framework of the hyperbolic model, in the Dirichlet problem only the thermal relaxation time and thermal diffusivity can be determined, simultaneously; however, in the Neumann problem, in addition to these thermal properties, the thermal effusivity and conductivity can also be observed. This fact represents a remarkable advantage of the Neumann problem with respect to the Dirichlet problem.

3.2 Effective Thermal Properties of a Layered System

The methodology presented in Sect. 3.1 can be useful to determine the thermal properties of a given material in the form of a sufficiently thick layer. However, when that layer is in thermal contact with other layers of different thermal properties (see Fig. 1c), as usually happens in technological applications, it is more convenient to determine effective thermal properties. In this case it is assumed that the layered system (Fig. 1c) can be understood as a one-layer system (Fig. 1b). This subsection is dedicated to
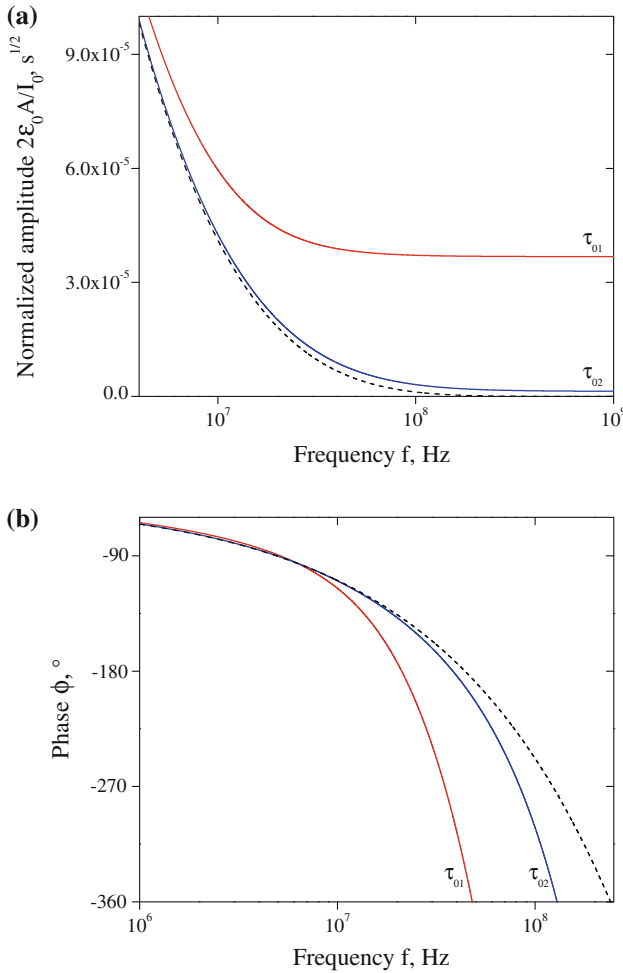
Fig. 4 (a) Normalized amplitude and (b) phase of the temperature as functions of the modulation frequency, for Neumann problem, taking $x = 2 \times 10^{-6}$ m and $\alpha_0 = 10^{-4}$ m$^2 \cdot$ s^{-1}. The *dashed line* corresponds to the parabolic model and the *solid lines* to the hyperbolic one for two values of τ_0: $\tau_{01} = 1 \times 10^{-8}$ s, $\tau_{02} = 1 \times 10^{-9}$ s

obtain useful effective thermal properties for determining the thermal properties of a finite layer (see Fig. 1c) when the thermal properties of the other layers are known.

3.2.1 Dirichlet Problem

Since $p_1 l_1 = \left(\chi_1 + i\chi_1^{-1}\right) l_1 / \mu_1$, then

$$\left| e^{-q_1 l_1} \right| = e^{-\frac{\chi_1 l_1}{\mu_1}}. \tag{28}$$

From the analysis of the size of the quantity $\chi_1 l_1/\mu_1$ and in analogy with traditional thermal wave phenomena [44], an extension of the usual concept of the thermal diffusion length for parabolic thermal waves μ_1 to a new quantity μ_1/χ_1 (the hyperbolic thermal conduction length) is necessary. In this way, the solutions given by Eq. 14 can be classified as thermally thin (for a layer such that $\chi_1 l_1/\mu_1 \ll 1$) and thermally thick (for a layer such that $\chi_1 l_1/\mu_1 \gg 1$). This will be crucial in the comprehension and analyses of hyperbolic heat transport phenomena, providing useful and convenient approximations of Eq. 14.

- For a thermally thin layer ($\chi_1^{-1} l_1/\mu_1 \ll 1$, which implies that $\chi_1 l_1/\mu_1 \ll 1$, because $\chi_1 \le 1$), Eq. 14 takes the form,

$$\theta(x) \approx \Theta e^{-\lambda_0 \left(\frac{p_1 l_1}{\lambda_1} + R_{10} \right)} e^{-p_0(x-l_1)}. \tag{29}$$

- In the case of a thermally thick layer ($\chi_1 l_1/\mu_1 \gg 1$, which implies that $\chi_1^{-1} l_1/\mu_1 \gg 1$, because $\chi_1^{-1} \ge 1$), Eq. 14 reduces to

$$\theta(x) \approx \Theta \left(\frac{2}{1 + \lambda_{01} + R_{10}\lambda_0} \right) e^{-p_1 l_1} e^{-p_0(x-l_1)}, \tag{30}$$

from which is obtained that $\theta(l_1) \approx \Theta[2/(1 + \lambda_{01} + R_{10}\lambda_0)] e^{-q_1 l_1}$. Comparing this equation with Eq. 13, for a semi-infinite medium, it can be observed that they are similar and only differ by the interface factor $2/(1 + \lambda_{01} + R_{10}\lambda_0)$ which is a consequence of the insertion of layer 1 in contact with the semi-infinite layer.

In analogy with the previous system, the approximations of Eq. 16 when both layers are thermally thin or thermally thick can be made as follows:

- For thermally thin layers ($\chi_j^{-1} l_j/\mu_j \ll 1$, $j = 1, 2$), Eq. 16 can be written as

$$\theta(x) \approx \Theta e^{-\lambda_0 \left(\frac{p_1 l_1}{\lambda_1} + \frac{p_2 l_2}{\lambda_2} + R_{12} + R_{20} \right)} e^{-p_0(x-l)}. \tag{31}$$

If it is considered that the two finite layers of thicknesses l_1 and l_2 behave as if they were a single one (the effective layer) of thickness $l = l_1 + l_2$, effective thermal conductivity k, and effective thermal relaxation time τ, according to Eq. 29, the temperature in this layer can be written in the form,

$$\theta(x) \approx \Theta e^{-\lambda_0 \left(\frac{pl}{\lambda} + R_{20} \right)} e^{-p_0(x-l)}. \tag{32}$$

Comparing Eqs. 31 and 32, it is obtained that

$$\frac{l}{k} = \frac{l_1}{k_1} + \frac{l_2}{k_2} + R_{12}, \tag{33a}$$

$$\tau \frac{l}{k} = \tau_1 \frac{l_1}{k_1} + \tau_2 \frac{l_2}{k_2}. \tag{33b}$$

Equation 33a has been previously obtained by Dramicanin et al. [24]; in the absence of an interface thermal resistance, it reduces to the formula determined by Lucio et al. [26], which is widely used in thermal characterization [26,27,36] under the framework of the parabolic model of heat conduction. Here, it is proved that Eq. 41 is not only true in the parabolic model but also in the hyperbolic model and is independent of the relaxation time of the component layers.

After dividing Eq. 33b by Eq. 33a, the following equation is obtained:

$$\tau = \frac{\tau_1 \frac{l_1}{k_1} + \tau_2 \frac{l_2}{k_2}}{\frac{l_1}{k_1} + \frac{l_2}{k_2} + R_{12}}, \tag{34}$$

which establishes that the effective thermal relaxation time is a weighted average of the thermal relaxation times of each layer, with the thermal resistances as the weights.

Solving the condition for thermally thin layers ($\chi_j^{-1} l_j / \mu_j \ll 1, j = 1, 2$), it can be shown that Eqs. 33a and 33b are valid for frequencies that satisfy

$$\omega \ll \frac{\omega_{cj}}{\sqrt{1 + 2\omega_{cj}\tau_j}}, \tag{35}$$

where $\omega_{cj} = 2\alpha_j / l_j^2$ is the classical cutoff frequency of the layer $j = 1, 2$ [3,13].

- For thermally thick layers ($\chi_j l_j / \mu_j \gg 1, j = 1, 2$), Eq. 16 is expressed as

$$\theta(x) \approx \Theta \left(\frac{2}{1 + \lambda_{02} + R_{20}\lambda_0} \right) \left(\frac{2}{1 + \lambda_{21} + R_{12}\lambda_2} \right) e^{-(p_1 l_1 + p_2 l_2)} e^{-p_0(x-l)}. \tag{36}$$

Considering again that the two finite layers of thicknesses l_1 and l_2 behave as if they were a single effective layer of thickness $l = l_1 + l_2$ and effective thermal diffusivity α; according to Eq. 30 and the remark made after it, the temperature in this layer can be written in the form,

$$\theta(x) \approx \Theta \left(\frac{2}{1 + \lambda_{02} + R_{20}\lambda_0} \right) e^{-pl} e^{-p_0(x-l)}. \tag{37}$$

Comparing Eqs. 36 and 37, it can be shown that

$$\chi \frac{l}{\sqrt{\alpha}} = \chi_1 \frac{l_1}{\sqrt{\alpha_1}} + \chi_2 \frac{l_2}{\sqrt{\alpha_2}} + \sqrt{\frac{2}{\omega}} \ln \left[\frac{1}{2} |1 + \lambda_{21} + R_{12}\lambda_2| \right], \tag{38}$$

where χ is given by Eq. 9c for the effective thermal relaxation time τ. Assuming that the effective thermal relaxation time does not vary appreciably with the modulation frequency, it is given by Eq. 34. It is important to remark that this effective parameter can also be determined using the amplitude A_{ef} and phase ϕ_{ef} of the effective thermal

signal expressed in Eq. 38. By defining $c \equiv [\ln(A_{\text{ef}}/\Theta)]'/(\phi_{\text{ef}})'$, where the prime (') indicates a derivative with respect to the thickness $l = l_1 + l_2$, it is shown that

$$\tau = \frac{c^{-1} - c}{4\pi f}, \tag{39}$$

In this way, the effective thermal relaxation time can be determined by measuring the quantity c for a given frequency or a set of them, inside the range defined for thermally thick layers ($\chi_j l_j/\mu_j \gg 1$), which is defined by

$$\omega \gg \frac{\omega_{cj}}{\sqrt{1 - 2\omega_{cj}\tau_j}}, \tag{40}$$

where $\omega_{cj} = 2\alpha_j/l_j^2$ is the classical cutoff frequency of the layer $j = 1, 2$ [3,13]. Notice that the denominator of Eq. 40 establishes a restriction for the thermal relaxation time given by

$$\tau_j < \frac{l_j^2}{4\alpha_j}, \tag{41}$$

which indicates that for a layer of thermal diffusivity α_j and thickness l_j, its thermal relaxation time has a least upper bound, proportional and very close to the thermalization time, obtained in the analysis of thermal transients [3]. This constraint establishes a limit for the validity of the hyperbolic model in the analysis of thermal transport that is closely connected with the consideration of heat transport as a collective motion.

To understand the predictions of Eq. 38, different limiting cases are considered:

- If the thermal relaxation times of each layer are zero ($\tau_1 = \tau_2 = \tau = 0$), corresponding to the parabolic limit of the CV equation, Eq. 38 reduces to

$$\frac{l}{\sqrt{\alpha}} = \frac{l_1}{\sqrt{\alpha_1}} + \frac{l_2}{\sqrt{\alpha_2}} + \frac{1}{\sqrt{\pi f}} \ln\left[\frac{1}{2}\sqrt{\left(1 + \frac{\varepsilon_2}{\varepsilon_1} + \varepsilon_2 R_{12}\sqrt{\pi f}\right)^2 + (\varepsilon_2 R_{12})^2 \pi f}\right]. \tag{42}$$

In the absence of the interface thermal resistance, Eq. 42 was first derived by Lucio et al. [26] for the same boundary conditions and under the framework of the Fourier law and it also reduces to a previous one derived by Tominaga and Ito [27] in the limit $f \to \infty$. Lucio et al. [26] have shown that the f-dependent term is necessary to explain previously reported experimental data [24,25], for a frequency range in which the individual layers are thermally thick in the traditional definition $\left(l_j/\mu_j \gg 1\right)$ of the Rosencwaig theory [44]. Therefore, under the framework of the parabolic model, the Lucio et al. result is a particular case of Eq. 42, which takes into account the interface thermal resistance between adjacent layers, and represents the parabolic limit of Eq. 38, valid in the framework of the hyperbolic model [26].

- For frequencies not so high, in such a way that $\omega_j \tau_j / \sqrt{1 - 2\omega_j \tau_j} \ll \omega \tau_j \ll 1$ for $j = 1, 2$ and performing a first-order approximation in $\omega \tau_j$, it can be shown that Eq. 38 can be written as

$$\frac{l(1 - \pi f \tau)}{\sqrt{\alpha}} = \frac{l_1(1 - \pi f \tau_1)}{\sqrt{\alpha_1}} + \frac{l_2(1 - \pi f \tau_2)}{\sqrt{\alpha_2}}$$
$$+ \frac{1}{\sqrt{\pi f}} \ln \left[\frac{1}{2} \sqrt{\left(1 + \frac{\varepsilon_2}{\varepsilon_1} + \varepsilon_2 R_{12} \sqrt{\pi f} \right)^2 + (\varepsilon_2 R_{12})^2 \pi f} \right]. \tag{43}$$

This expression is similar to that obtained in the parabolic approximation (Eq. 42); in fact, the logarithmic part is the same. However, the effective thermal diffusivity is slightly different, due to the weak dependence on the thermal relaxation times.

- For high modulation frequencies in which the condition $\omega \tau_j \gg \max \left\{ 1, \omega_j \tau_j / \sqrt{1 - 2\omega_j \tau_j} \right\}$ for $j = 1, 2$ is fulfilled, and for an approximation of first order in $(\omega \tau_j)^{-1}$, the following expression is obtained from Eq. 39:

$$\frac{l}{\sqrt{\alpha \tau}} = \frac{l_1}{\sqrt{\alpha_1 \tau_1}} + \frac{l_2}{\sqrt{\alpha_2 \tau_2}} + 2 \ln \left[\frac{1}{2} \left(1 + \frac{\varepsilon_2}{\varepsilon_1} \sqrt{\frac{\tau_1}{\tau_2}} + \frac{\varepsilon_2 R_{12}}{\sqrt{\tau_2}} \right) \right]. \tag{44}$$

which establishes that for very high frequencies, the hyperbolic effective thermal diffusivity is independent of the modulation frequency, and represents the hyperbolic generalization of the Tominaga and Ito formula [35].

3.2.2 Neumann Problem

Following a similar procedure for the analysis of the solutions obtained with the Neumann boundary conditions as the one used in the Dirichlet problem, and comparing the temperature of a system of one finite layer (Eq. 20) with the temperature of the system for two finite layers (Eq. 21), the following results are obtained:

- If both finite layers are thermally thin, it can be shown that

$$\rho c l = \rho_1 c_1 l_1 + \rho_2 c_2 l_2. \tag{45}$$

Since the quantity, with $\rho c l \Lambda$, with Λ being the common transversal area of the layers, represents the heat capacity of the effective layer, Eq. 45 is just an expected identity, due to the fact that this property is an extensive thermodynamic variable. This result has also been obtained previously based on the parabolic model for conventional thermal wave phenomena using the same boundary conditions [28]. In this way, for thermally thin layers, under the framework of the parabolic or hyperbolic models, and obeying Neumann boundary conditions, it is not possible to obtain a useful formula for the effective thermal properties of a layered system. This result

is in strong contrast with Eq. 33a for the effective thermal conductivity obtained using the Dirichlet boundary conditions in the parabolic and hyperbolic models and under steady-state boundary conditions. Given the characteristics of the boundary conditions, in the limit when the frequency goes to zero, Neumann conditions imply an asymptotically increasing deposition of thermal energy on the sample surface. This is not consistent with steady-state conditions that guarantee the validity of the equation for the effective thermal conductivity given by Eq. 33a. Therefore, the heat capacity identity obtained in Eq. 45 for the Neumann boundary condition is only a consistency equation that must be expected to be fulfilled.

- If both layers are thermally thick, for Neumann boundary conditions the same formula found in the Dirichlet problem (Eq. 38) is obtained, where the effective thermal relaxation time can still be determined using Eq. 39. This indicates that in an experiment dedicated to measure the effective thermal properties, for high modulation frequencies, it is equivalent to establishing a temperature or a heat flux boundary condition as the excitation source at the surface $x = 0$ of the first layer.

4 Analysis and Discussion

In this section, the predictions of the obtained equations for the effective thermal properties are explored by comparing with conventional parabolic results. Typical values for thermal diffusivities, the thickness, and thermal relaxation times reported in the literature for crystal solids are used (see Table 1) [10]. Given that for thermally thin layers, parabolic and hyperbolic approaches provide the same results, only the case in which both layers are thermally thick is going to be analyzed.

Under the framework of the parabolic model, in Fig. 5a and b the effective thermal diffusivity as a function of the modulation frequency is shown for the corresponding values of the properties given in Table 1. In this case both composing layers are thermally thick for high frequencies ($f \gg 6.5 \times 10^5$ Hz) in which Eq. 42 is valid. Figure 5a shows that in the absence of an interface thermal resistance ($R_{12} = 0$), the effective thermal diffusivity is always smaller than the larger thermal diffusivity of the component layers, being a maximum when the first layer is a perfect thermal conductor ($\varepsilon_2/\varepsilon_1 = 0$) and a minimum when the first layer is a perfect thermal insulator ($\varepsilon_2/\varepsilon_1 \to \infty$). Note that for extremely high frequencies, the curves of the effective thermal diffusivity converge to the horizontal limit line ($\varepsilon_2/\varepsilon_1 = 1$), with an effective thermal diffusivity $= 0.628$ cm$^2 \cdot$s^{-1}.

Figure 5b shows that, under the framework of the parabolic approach, for fixed values of the thermal effusivities of the component layers, the effective thermal diffusivity decreases remarkably when the interface thermal resistance increases, and becomes

Table 1 Thermal and geometrical properties of layers 1 and 2

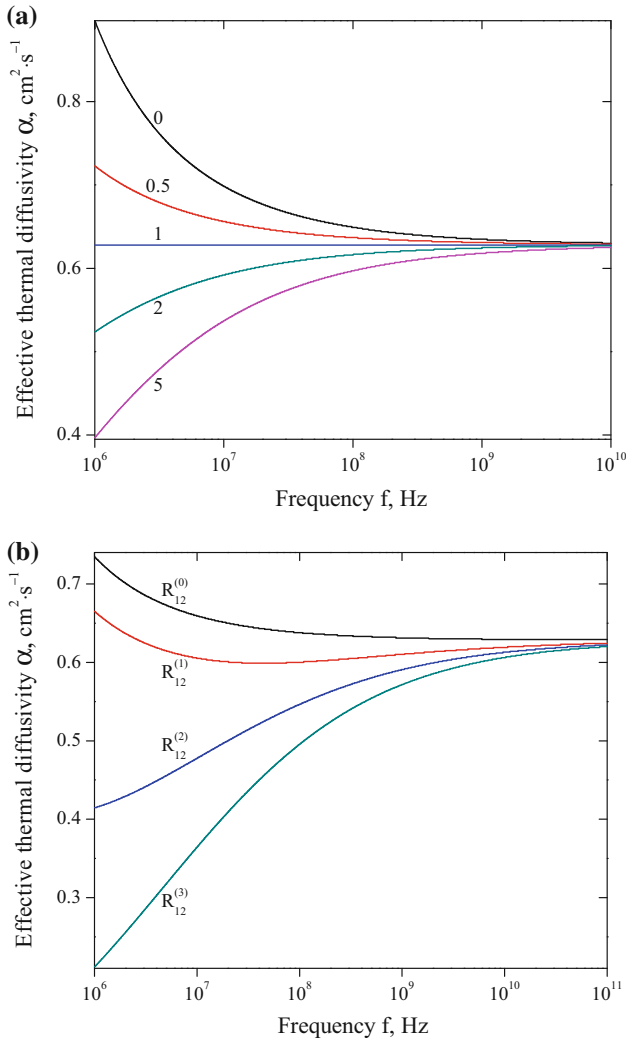| α_1 (cm$^2 \cdot$s^{-1})	α_2 (cm$^2 \cdot$s^{-1})	ε_1 (W$\cdot$s$^{1/2} \cdot$m$^{-2} \cdot$K^{-1})	ε_2 (W$\cdot$s$^{1/2} \cdot$m$^{-2} \cdot$K^{-1})	τ_1 (ηs)	τ_2 (ηs)	l_1 (μm)	l_2 (μm)
1	0.5	37137	16797	5	1	7	12

Fig. 5 Effective thermal diffusivity predicted by the parabolic model for a system of thermally thick layers as a function of the modulation frequency, taking (a) different values of the ratio of thermal effusivities $\varepsilon_2/\varepsilon_1$ of the composing layers and $R_{12} = 0$, and (b) different values of the interface thermal resistance R_{12}: $R_{12}^{(0)} = 0$, $R_{12}^{(1)} = 10^{-8}\,\text{m}^2 \cdot \text{K} \cdot \text{W}^{-1}$, $R_{12}^{(2)} = 10^{-7}\,\text{m}^2 \cdot \text{K} \cdot \text{W}^{-1}$, and $R_{12}^{(3)} = 10^{-6}\,\text{m}^2 \cdot \text{K} \cdot \text{W}^{-1}$

independent of the modulation frequency and of the interface thermal resistance for sufficiently high frequencies. These facts indicate that for frequencies not so high, inside the interval of thermally thick layers, the interface thermal resistance plays an important role in the process of heat conduction [26–28,35,36].

For the hyperbolic model, in Fig. 6a and b, the effective thermal diffusivity is shown as a function of the modulation frequency, for different values of the ratio of thermal effusivities $\varepsilon_2/\varepsilon_1$, in the absence of the interface thermal resistance ($R_{12} = 0$) and
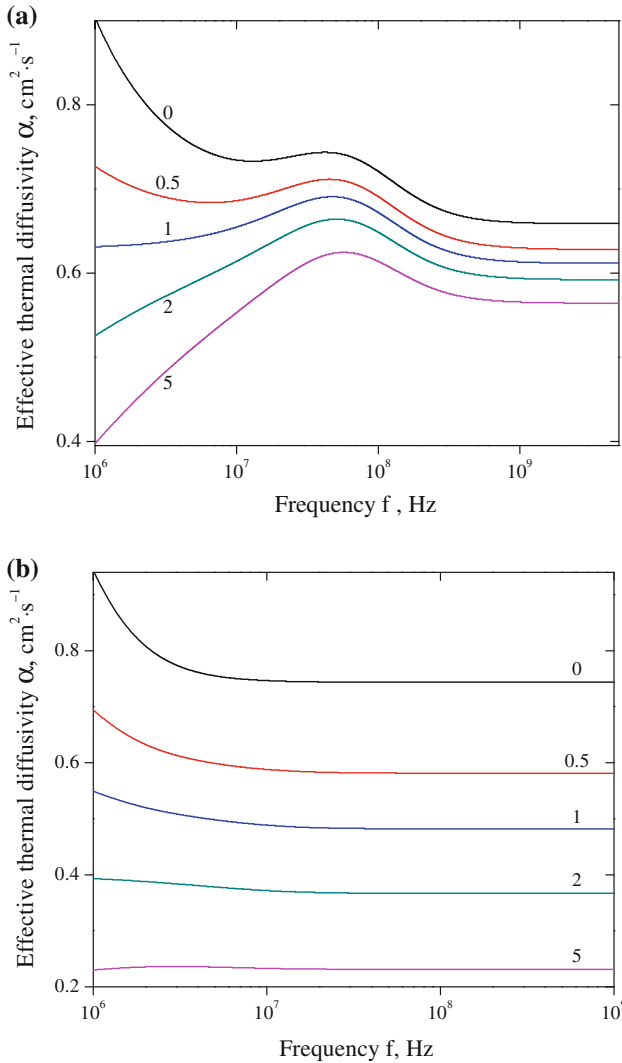
Fig. 6 Effective thermal diffusivity predicted by the hyperbolic model for a system of thermally thick layers as a function of the modulation frequency, taking different values of the ratio of thermal effusivities $\varepsilon_2/\varepsilon_1$ of the component layers and $R_{12} = 0$: (a) for values of the thermal relaxation times given in Table 1 and (b) for thermal relaxation times: $\tau_1 = 1.1 \times 10^{-7}$ s and $\tau_2 = 7.1 \times 10^{-7}$ s, which are close to their least upper bound given in Eq. 36

the corresponding values of the properties given in Table 1. Both component layers are thermally thick for high frequencies such that $f \gg 6.6 \times 10^5$ Hz for the case of Fig. 6a, and $f \gg 2.0 \times 10^6$ Hz, for Fig. 6b in which Eq. 39 is valid.

In Fig. 6a it is shown that for the thermal relaxation times of the component layers given in Table 1, which are not close to their least upper bounds (see Eq. 41: $\tau_1 < 1.2 \times 10^{-7}$ s and $\tau_2 < 7.2 \times 10^{-7}$ s, the effective thermal diffusivity decreases when

the ratio $\varepsilon_2/\varepsilon_1$ of thermal effusivities increases. This is a similar behavior to the one presented for the parabolic model in Fig. 5a; however, in contrast to the prediction of this model, in the hyperbolic approach the effective thermal diffusivity has a local maximum value, and for sufficient high modulation frequencies, it tends to a frequency-independent value, being larger for lower values of the ratio $\varepsilon_2/\varepsilon_1$ of thermal effusivities. This is due to the fact that for too high frequencies the logarithmic term in Eq. 38 does not vanish, but rather takes the form given in Eq. 44.

Figure 6b shows that for the thermal relaxation times of the component layers, close to their least upper bounds (see Eq. 41: $\tau_1 < 1.2 \times 10^{-7}$s and $\tau_2 < 7.2 \times 10^{-7}$s, the effective thermal diffusivity is almost independent of the modulation frequency and takes different values for different values of the ratio $\varepsilon_2/\varepsilon_1$ of thermal effusivities. This fact reveals that the changes presented by the effective thermal diffusivity in Fig. 6a are attenuated when the thermal relaxation times of the component layers tend to their corresponding least upper bounds. It can be shown that for thermal relaxation times larger than their corresponding least upper bounds, the effective thermal diffusivity can increase without limit. This indicates that the constraint given in Eq. 41 must be taken into account in order to get physically reasonable results.

In Fig. 7a and b the effective thermal diffusivity as a function of the modulation frequency is shown, for different values of the interface thermal resistance and the corresponding values of the properties given in Table 1. In this case, both component layers are thermally thick for frequencies such that $f \gg 6.6 \times 10^5$ Hz. Figure 7a shows that for fixed values of the thermal effusivities of the composing layers, the effective thermal diffusivity takes lower values when the interface thermal resistance increases, and becomes independent of the modulation frequency for sufficiently high frequencies. However, in contrast to the predictions of the parabolic model, the hyperbolic effective thermal diffusivity depends on the interface thermal resistance for too high frequencies, such as established by Eq. 44. This last fact is shown in Fig. 7b, where the parabolic effective thermal diffusivity (dashed lines) tends to a value independent of both the modulation frequency and the interface thermal resistance, for sufficiently high frequencies; while in the hyperbolic model, it becomes independent of the modulation frequency but continues depending on the interface thermal resistance.

After expressing $\theta(x = l)$ in Eq. 37 as a complex number in its polar form, it can be shown that its amplitude is given by

$$A(f) = \Theta \frac{2}{|1 + \lambda_{02} + R_{20}\lambda_0|} \frac{2}{|1 + \lambda_{21} + R_{12}\lambda_2|} e^{-\sqrt{\pi f}\left(\frac{\chi_1 l_1}{\sqrt{\alpha_1}} + \frac{\chi_2 l_2}{\sqrt{\alpha_2}}\right)}, \qquad (46)$$

which indicates that the interface thermal resistance attenuates the amplitude as was expected. In Fig. 8, the normalized amplitude is shown as a function of the modulation frequency, for the corresponding properties of the two finite layers given in Table 1, and taking $\varepsilon_0 = 1500 \ \mathrm{W \cdot s^{1/2} \cdot m^{-2} \cdot K^{-1}}$, $\tau_0 = 3 \times 10^{-8}$ s, and $R_{20} = 5 \times 10^{-8} \ \mathrm{m^2 \cdot K \cdot W^{-1}}$, for the semi-infinite layer. Calculations have been made considering two values of the interface thermal resistance R_{12}: $R_{12}^{(0)} = 0$ and $R_{12}^{(1)} = 10^{-7} \ \mathrm{m^2 \cdot K \cdot W^{-1}}$. In this case, both layers are thermally thick for frequencies such that $f \gg 6.6 \times 10^5$ Hz, where Eq. 46 is valid.
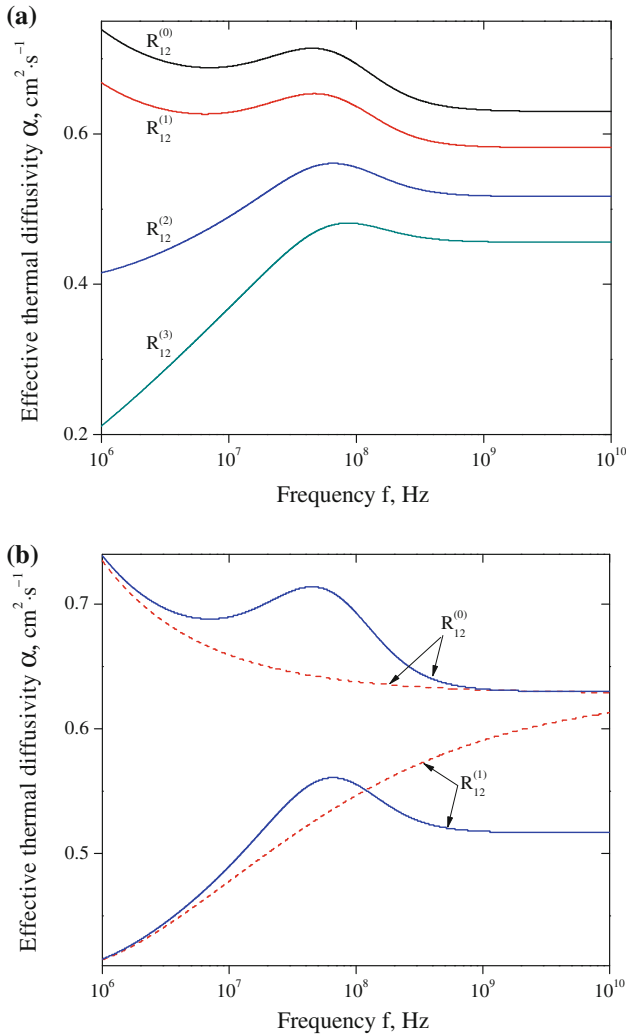
Fig. 7 Effective thermal diffusivity predicted by the hyperbolic model for a system of thermally thick layers as a function of the modulation frequency, for the thermal properties given in Table 1, and taking different values of the interface thermal resistance R_{12}: (a) $R_{12}^{(0)} = 0$, $R_{12}^{(1)} = 10^{-8}\,\mathrm{m^2 \cdot K \cdot W^{-1}}$, $R_{12}^{(2)} = 10^{-7}\,\mathrm{m^2 \cdot K \cdot W^{-1}}$, and $R_{12}^{(3)} = 10^{-6}\,\mathrm{m^2 \cdot K \cdot W^{-1}}$ and (b) $R_{12}^{(0)} = 0$ and $R_{12}^{(1)} = 10^{-7}\,\mathrm{m^2 \cdot K \cdot W^{-1}}$. The predictions of the parabolic model are shown by *dashed lines*

Figure 8 shows that:

- When the interface thermal resistance (R_{12}) between the finite layers is taken into account $\left(R_{12}^{(1)} = 10^{-7}\,\mathrm{m^2 \cdot K \cdot W^{-1}} \right)$, the normalized amplitude predicted by both parabolic and hyperbolic models is reduced remarkably with respect to the one in the absence of an interface thermal resistance ($R_{12}^{(0)} = 0$). This fact establishes that for the whole interval of frequencies, in which both finite layers are thermally thick,
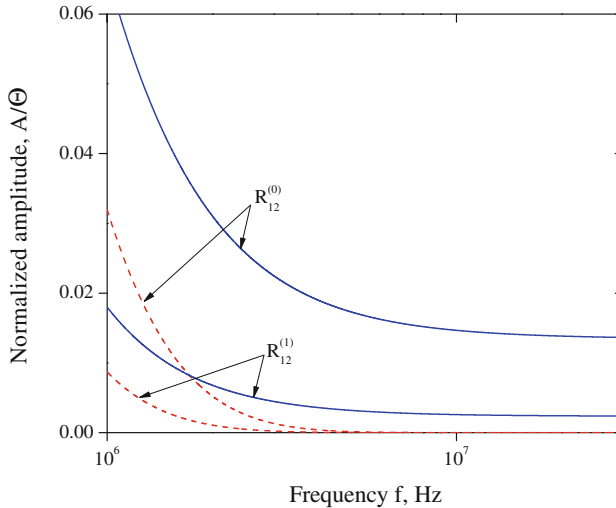
Fig. 8 Normalized amplitude of the temperature as functions of the modulation frequency, for the Dirichlet problem and the corresponding properties given in Table 1. The *dashed lines* correspond to the parabolic model and the *solid lines* to the hyperbolic one for two values of the interface thermal resistance R_{12}: $R_{12}^{(0)} = 0$ and $R_{12}^{(1)} = 10^{-7} \, \mathrm{m^2 \cdot K \cdot W^{-1}}$, with $\varepsilon_0 = 1500 \, \mathrm{W \cdot s^{1/2} \cdot m^{-2} \cdot K^{-1}}$, $\tau_0 = 3 \times 10^{-8} \, \mathrm{s}$, and $R_{20} = 5 \times 10^{-8} \mathrm{m^2 \cdot K \cdot W^{-1}}$

the interface thermal resistance is a determinant parameter in the process of heat conduction and it has to be considered in practical applications of thin films.

- Inside the whole interval of frequencies for which both finite layers are thermally thick, the normalized amplitude predicted by the hyperbolic model is larger than the corresponding one predicted by the parabolic model. This could be expected, given that the wave-like form of the hyperbolic heat conduction equation permits an enhancement of the heat transfer as compared with the purely diffusive parabolic behavior predicted by Fourier's law.

- For higher frequencies $\left(\omega \tau_j \gg 1, \, j = 1, 2\right)$ in the range of thermally thick layers, for the hyperbolic model, the amplitude becomes independent of the modulation frequency while in the parabolic model, it tends to zero. This indicates that for this range of frequencies the hyperbolic thermal waves can travel larger distances than those predicted by the parabolic model and that the thermal waves established by the hyperbolic model at the fixed position are always present, no matter how high is the modulation frequency. This could be useful in the evaluation of the role of hyperbolic effects in systems where abnormally high thermal properties have been reported, in contradiction with the values predicted by the traditional mean field theories based on Fourier's law [5,22].

- It is important to note that when the thermal relaxation times are changed, restricted to values allowed by Eq. 36, it is straightforward to show that the difference between the results obtained from the parabolic and hyperbolic models decreases when the thermal relaxation times of each layer move away from their corresponding least

upper bounds and become negligible when the thermal relaxation times of each layer tend to zero.

5 Effective Thermal Conductivity and Thermal Diffusivity of N Finite Layers

The generalization of Eqs. 33a and 38, for the effective thermal conductivity and thermal diffusivity of two finite layers can be easily performed for a system of $N \geq 2$ finite layers. Solving the Dirichlet problem (Eq. 12) with the boundary conditions given in Eqs. 11a and 11b, it is only necessary to obtain the spatial part $\theta(x)$ of the oscillatory component of the temperature for $x \geq l = l_1 + l_2 + \cdots + l_N$, where l_n is the thickness of the layer $n = 1, 2, ..., N$. Following a similar procedure as the one presented in Sect. 3.2.1, the following results are obtained:

- For thermally thin layers ($\chi_n^{-1} l_n / \mu_n \gg 1$, $n = 1, 2, ..., N$),

$$\frac{l}{k} = \sum_{n=1}^{N} \frac{l_n}{k_n} + \sum_{n=1}^{N-1} R_{n,n+1}, \tag{47}$$

and the thermal relaxation time of the effective layer is given by the weighted average

$$\tau = \frac{\sum_{n=1}^{N} \tau_n \frac{l_n}{k_n}}{\sum_{n=1}^{N} \frac{l_n}{k_n} + \sum_{n=1}^{N-1} R_{n,n+1}}. \tag{48}$$

- For thermally thick layers ($\chi_n l_n / \mu_n \gg 1$, $n = 1, 2, ..., N$),

$$\chi \frac{1}{\sqrt{\alpha}} = \sum_{n=1}^{N} \chi_n \frac{l_n}{\sqrt{\alpha_n}} + \sqrt{\frac{2}{\omega}} \ln \left[\frac{1}{2^{N-1}} \prod_{n-1}^{N-1} \left| 1 + \lambda_{n+1,n} + R_{n,n+1}\lambda_{n+1} \right| \right], \tag{49}$$

whose parabolic limit is

$$\frac{l}{\sqrt{\alpha}} = \sum_{n=1}^{N} \frac{l_n}{\sqrt{\alpha}}$$
$$+ \sqrt{\frac{2}{\omega}} \ln \left[\frac{1}{2^{N-1}} \prod_{n-1}^{N-1} \sqrt{\left(1 + \frac{\varepsilon_{n+1}}{\varepsilon_n} + R_{n,n+1}\varepsilon_{n+1}\sqrt{\pi f} \right)^2 + \left(R_{n,n+1}\varepsilon_{n+1} \right)^2 \pi f} \right]. \tag{50}$$

The presented results for the effective thermal properties can be used as the basis in the development of more general formulas for the analysis of thermal properties, under the framework of generalized models of heat conduction such as the dual-phase lag model [8,14,15,45–48] when the interface thermal resistance between adjacent layers is considered.

6 Conclusions

Thermal wave transport in a layered system was analyzed using the hyperbolic model of heat conduction and considering a modulated thermal excitation at the surface with Dirichlet and Neumann boundary conditions. For a single semi-infinite layer, useful and analytical formulas to determine its thermal relaxation time as well as additional thermal properties have been found. For a system of two finite layers in thermal contact with a semi-infinite one, under the Dirichlet boundary condition, formulas for the effective thermal conductivity and the effective thermal relaxation time have been obtained, when both component layers are thermally thin. In contrast in the thermally thick regime, an analytical expression for both Dirichlet and Neumann conditions has been obtained for the effective thermal diffusivity of the two finite layers in terms of their thermal properties and their interface thermal resistance. It has been demonstrated that our formulas reduce to known parabolic results when the thermal relaxation times of all layers are zero and can be used in the thermal characterization of the component layers. In addition, it has been shown that the interface thermal resistance may reduce remarkably the amplitude of the thermal signal in the process of heat conduction and, therefore, it has to be taken into account for most of the theoretical approaches and experimental conditions. In this way, our results can be used to interpret and analyze experimental results and theoretical models of complex layered systems establishing the basis for the development of more general formulas under the framework of generalized models.

References

1. S. Torquato, *Random Heterogeneous Materials* (Springer-Verlag, New York, 2001)
2. H.S. Carslaw, J.C. Jaeger, *Conduction of Heat in Solids* (Oxford University Press, London, 1959)
3. W.P. Leung, A.C. Tam, J. Appl. Phys. **56**, 153 (1984)
4. S.U.S. Choi, Z.G. Zhang, W. Yu, F.E. Lockwood, E.A. Grulke, Appl. Phys. Lett. **79**, 2252 (2001)
5. J.A. Eastman, S.U.S. Choi, S. Li, W. Yu, L.J. Thompson, Appl. Phys. Lett. **78**, 718 (2001)
6. W. Kaminski, ASME J. Heat Transf. **112**, 555 (1990)
7. D.D. Joseph, L. Preziosi, Rev. Mod. Phys. **61**, 41 (1989)
8. D.Y. Tzou, *Macro- to Microscale Heat Transfer: The Lagging Behavior* (Taylor and Francis, New York, 1997)
9. R.K. Sahoo, Cryogenics **34**, 203 (1994)
10. A. Vedavarz, S. Kumar, M.K. Moallemi, ASME J. Heat Transf. **116**, 221 (1994)
11. C. Cattaneo, Atti. Semin. Mat. Fis. Univ. Modena **3**, 83 (1948)
12. P. Vernotte, C.R. Hebdomadaires des Seances de l'Academie des Sciences **246**, 3154 (1958)
13. M.N. Ozisik, D.Y. Tzou, ASME J. Heat Transf. **116**, 526 (1994)
14. D.Y. Tzou, J. Thermophys. Heat Transf. **9**, 686 (1995)
15. D.Y. Tzou, ASME J. Heat Transf. **117**, 8 (1995)
16. J.-R. Ho, C.-P. Kuo, W.-S. Jiaung, Int. J. Heat Mass Transf. **46**, 55 (2003)
17. S. Galovic, D. Kotoski, J. Appl. Phys. **93**, 3063 (2003)
18. L. Wang, X. Zhou, X. Wei, *Heat Conduction: Mathematical Models and Analytical Solutions* (Springer-Verlag, Berlin, Heidelberg, 2008)
19. W. Roetzel, N. Putra, S.K. Das, Int. J. Therm. Sci. **42**, 541 (2003)
20. K. Mitra, S. Kumar, A. Vedavarz, M.K. Moallemi, ASME J. Heat Transf. **117**, 568 (1995)
21. L. Cheng, M.T. Xu, L.Q. Wang, Int. J. Heat Mass Transf. **51**, 6018 (2008)
22. J.J. Vadasz, S. Govender, P. Vadasz, Int. J. Heat Mass Transf. **48**, 2673 (2005)
23. M.A. Al-Nimr, M. Naji, R.I. Abdallah, Int. J. Thermophys. **25**, 949 (2004)

24. M.D. Dramicanin, Z.D. Ristovski, V. Djokovic, S. Galovic, Appl. Phys. Lett. **73**, 321 (1998)
25. A.F. Khadrawi, M.A. Al-Nimr, M. Hammad, Int. J. Thermophys. **23**, 581 (2002)
26. J.L. Lucio, J.J. Alvarado-Gil, O. Zelaya-Angel, H. Vargas, Phys. Status Solidi A **150**, 695 (1995)
27. A.M. Mansanares, H. Vargas, F. Galembeck, J. Buijs, D. Bicanic, J. Appl. Phys. **70**, 7046 (1991)
28. E. Marin, J.L. Pichardo, A. Cruz-Orea, P. Diaz, G. Torres-Delgado, I. Delgadillo, J.J. Alvarado-Gil, J.G. Mendoza-Alvarez, H. Vargas, J. Phys. D: Appl. Phys. **29**, 981 (1996)
29. W.B. Lor, H.S. Chu, Int. J. Heat Mass Transf. **43**, 653 (2000)
30. J. Ordóñez-Miranda, J.J. Alvarado-Gil, ASME J. Heat Transf. (2010). doi:10.1115/1.4000748
31. K. Ramadan, Int. J. Therm. Sci. **48**, 14 (2009)
32. K. Ramadan, M.A. Al-Nimr, ASME J. Heat Transf. **130**, 074501 (2008)
33. K. Ramadan, M.A. Al-Nimr, Heat Transf. Eng. **30**, 677 (2009)
34. K. Ramadan, M.A. Al-Nimr, Int. J. Therm. Sci. **48**, 1718 (2009)
35. T. Tominaga, K. Ito, Jpn. J. Appl. Phys. **27**, 2392 (1988)
36. A.M. Mansanares, A.C. Bento, H. Vargas, N.F. Leite, L.C.M. Miranda, Phys. Rev. B **42**, 4477 (1990)
37. A. Salazar, A. Sánchez-Lavega, J.M. Terrón, J. Appl. Phys. **84**, 3031 (1998)
38. J. Ordonez-Miranda, J.J. Alvarado-Gil, Int. J. Therm. Sci. **48**, 2053 (2009)
39. D.P. Almond, P.M. Patel, *Photothermal Science and Techniques* (Chapman and Hall, London, 1996)
40. F.A. Mcdonald, G.C. Westel, J. Appl. Phys. **49**, 2313 (1978)
41. J.L. Pichardo, J.J. Alvarado-Gil, J. Appl. Phys. **89**, 4070 (2001)
42. B.-C. Li, S.-Y. Zhang, J. Phys. D: Appl. Phys. **30**, 1447 (1997)
43. A. Salazar, Eur. J. Phys. **24**, 351 (2003)
44. A. Rosencwaig, A. Gersho, J. Appl. Phys. **47**, 64 (1976)
45. D.Y. Tzou, ASME J. Heat Transf. **111**, 232 (1989)
46. D.Y. Tzou, Int. J. Eng. Sci. **29**, 1167 (1991)
47. D.Y. Tzou, ASME J. Appl. Mech. **59**, 862 (1992)
48. D.Y. Tzou, J. Thermophys. Heat Transf. **16**, 30 (2002)